Bioorganic & Medicinal Chemistry Letters 21 (2011) 6505–6509

Contents lists available at SciVerse ScienceDirect

Bioorganic & Medicinal Chemistry Letters

journal homepage: www.elsevier.com/locate/bmcl

Conversion of systemically-distributed triazole-based stearoyl-CoA desaturase (SCD) uHTS hits into liver-targeted SCD inhibitors

Jean-Philippe Leclerc [a,*], Jean-Pierre Falgueyret [b], Mélina Girardin [c], Jocelyne Guay [b], Sébastien Guiral [b], Zheng Huang [b], Chun Sing Li [a], Renata Oballa [a], Yeeman K. Ramtohul [a], Kathryn Skorey [b], Paul Tawa [b], Hao Wang [b], Lei Zhang [b]

[a] Department of Medicinal Chemistry, Merck Frosst Centre for Therapeutic Research, 16711 TransCanada Hwy, Kirkland, Quebec, Canada H9H 3L1
[b] Department of Biochemistry and Molecular Biology, Merck Frosst Centre for Therapeutic Research, 16711 TransCanada Hwy, Kirkland, Quebec, Canada H9H 3L1
[c] Department of Process Research, Merck Frosst Centre for Therapeutic Research, 16711 TransCanada Hwy, Kirkland, Quebec, Canada H9H 3L1

ARTICLE INFO

Article history:
Received 21 June 2011
Revised 11 August 2011
Accepted 15 August 2011
Available online 25 August 2011

Keywords:
Stearoyl-CoA desaturase inhibitors
SCD inhibitors
Triazoles
Liver-targeted
MK-8245

ABSTRACT

It has been demonstrated that once-a-day dosing of systemically-distributed SCD inhibitors leads to adverse events in eye and skin. Herein, we describe our efforts to convert a novel class of systemically-distributed potent triazole-based uHTS hits into liver-targeted SCD inhibitors as a means to circumvent chronic toxicity.

Obesity and type II diabetes are two major health issues affecting predominantly western countries. New medicines targeting novel mechanism that may show advantages over existing medications are urgently needed.[1] Stearoyl-CoA desaturase (SCD) is an important enzyme involved in the lipogenic pathway. SCD, also known as delta-9 desaturase (Δ9D), catalyzes the initial desaturation of saturated long-chain fatty acids into monounsaturated fatty acids at their Δ9 position. More precisely, the favored SCD substrates are stearoyl-CoA and palmitoyl-CoA which are converted into oleoyl-CoA and palmitoleoyl-CoA, respectively.[2] These monosaturated fatty acids are the major components of various lipids such as phospholipids, triglycerides, cholesterol ester and wax esters.[3] Recent studies in rodents have shown that inhibition, mutation or deletion of SCD has a direct effect on fat utilization and storage, which results in insulin sensitivity improvement, resistance to diet-induced obesity, reduction of adiposity and plasma triglycerides levels.[4] Therefore, SCD represents an attractive new target which could lead to the discovery of novel treatments for obesity, type-2 diabetes and related metabolic disorders.[5]

We recently have disclosed the discovery of **MF-152**[6] and **MF-438**[7] (Fig. 1) for assay development and proof-of-concept studies in rodents. As part of our continued efforts to identify SCD inhibitors devoid of eye and skin adverse events, the SAR and optimization of a structurally diverse series of SCD inhibitors are described herein.

Several groups have reported a number of different small-molecules for the inhibition of the SCD enzyme.[8,9] To identify novel and new structurally distinct inhibitors in this area, an ultra high throughput screening (uHTS) campaign was undertaken.[10] Overall, 24 promising compounds were identified with IC_{50} values <300 nM. In particular, a class of structurally distinct potent triazole SCD inhibitors, as illustrated by **3** and **4** with IC_{50} values of 6 nM and 12 nM, respectively, were identified (Fig. 2). Structure activity explorations began with removal of the free amino group in **3,** leading to compound **5,** which is equipotent to the parent compound in the rat microsomal assay (rSCD enzyme).[11] For synthetic simplicity, further SAR studies were focused on the des-amino triazole moiety.

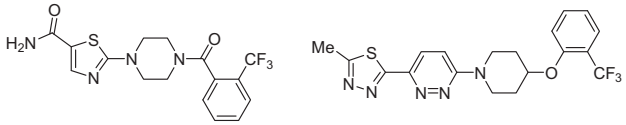

Figure 1. **MF-152** and **MF-438** for assay development and rodent proof-of-concept studies.

* Corresponding author.
E-mail address: j.philippe.leclerc@gmail.com (J.-P. Leclerc).

0960-894X/$ - see front matter © 2011 Elsevier Ltd. All rights reserved.
doi:10.1016/j.bmcl.2011.08.073

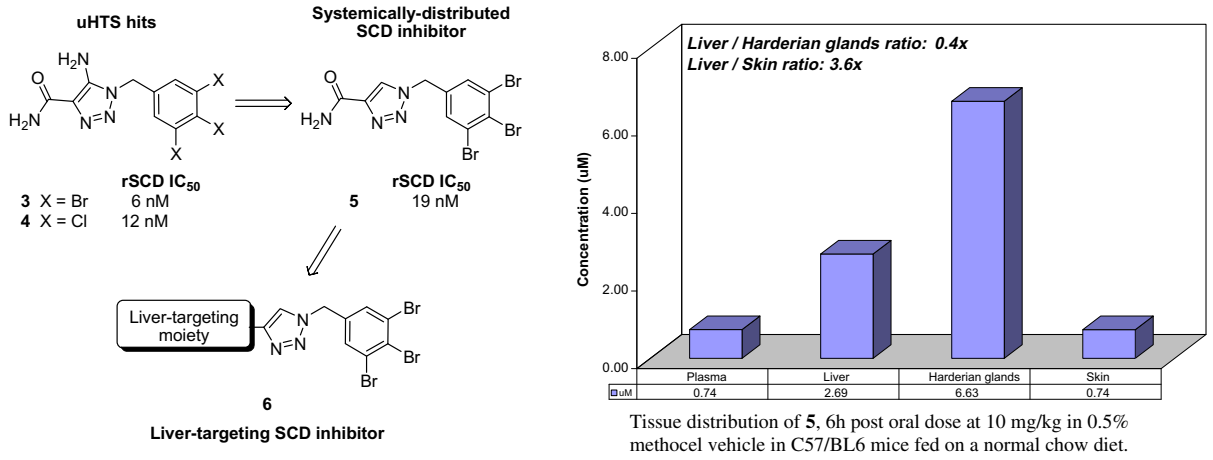

Figure 2. Strategy: Incorporation of a liver-targeting moiety on the systemic SCD inhibitor **5** derived from a uHTs campaign.

As expected, the tissue distribution profile of **5** (6 h post oral dose at 10 mg/kg in mouse) showed high exposures in many tissues and therefore confirmed that **5** was, indeed, systemically-distributed (Fig. 2).

As reported previously with **MF-152** and **MF-438,** systemically distributed compounds lead to the development of partial eye closure and progressive alopecia after ~7–14 days of drug treatment in rodents.[6,7] We believed that SCD inhibition in the eye-lubricating Harderian glands and skin leads to reduced levels of SCD-derived lipids present in the tears and skin/sebaceous glands which may be essential for eye lubrication and healthy skin. Therefore, we initially hypothesized that selectively targeting the liver (where the SCD enzyme is mainly expressed), would lead to efficient inhibitors with reduced eye and skin adverse events. Indeed, this supposition was confirmed by the design of the liver-targeted SCD inhibitor **MK-8245**.[12] This compound is actively transported inside the hepatocyte cells by the organic anion transporting polypeptides (OATPs)[13] which can recognize a carboxylic acid residue moiety present on the compound. Targeting OATPs favored the active transport of the compound into the hepatocyctes over the unselective passive cell diffusion. In light of these findings, we sought to apply the same strategy to convert uHTS hits into liver-targeted SCD inhibitors (Fig. 2).

Since the tetrazole acetic acid was believed to be the key moiety responsible for liver-targeting, we directly replaced the primary amide in **5** with this group. As show in Scheme 1,[14] the triazole

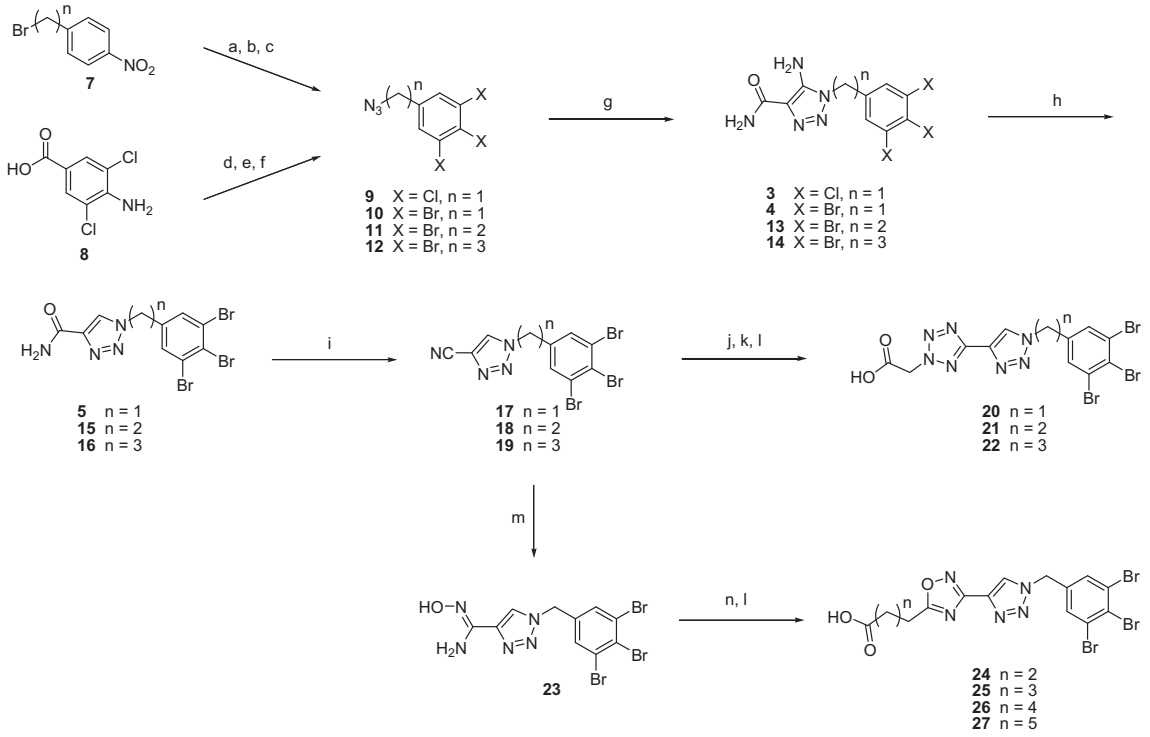

Scheme 1. Reagents and conditions: (a) Pd/C, H_2, rt, 5 h; (b) Br_2, $CuBr_2$, MeCN, 50 °C, 1 h, then *t*-BuONO, 0.5 h; (c) NaN_3, dimethyl formamide (DMF); (d) $LiAlH_4$, tetrahydrofurane (THF), 60 °C, 7 h; (e) *t*-BuONO, $CuCl_2$, MeCN, rt, 2 h; (f) $(PhO)_2PN_3$, DBU, toluene, rt, 3 h; (g) $H_2NC(O)CH_2CN$, NaOH, EtOH, 85 °C, 3 h; (h) *t*-BuONO, THF, 50 °C, 2 h; (i) TFAA, triethylamine (TEA), dichlormethane (DCM), rt, 2 h; (j) NaN_3, NH_4Cl, DMF, 105 °C, 2 h; (k) ethyl2-bromoacetate, TEA, THF, reflux, 2 h; (l) NaOH, THF, MeOH, rt, 3 h; (m) $NH_2OH{\cdot}HCl$, K_2CO_3, EtOH, rt, 16 h; (n) $EtOC(O)CH_2(CH_2)_nC(O)Cl$, pyridine, 90 °C, 20 h.

Table 1
Effect on linker's length

Compound	Structures		SCD IC_{50} (nM) Rat microsomal[a]
3	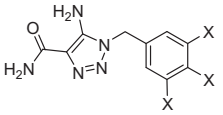	X = Br	6
4		X = Cl	12
5	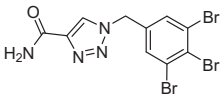		19
20	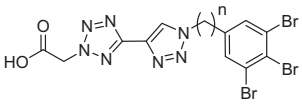	*n* = 1	>20,000
21		*n* = 2	19,900
22		*n* = 3	911
24	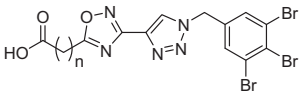	*n* = 2	552
25		*n* = 3	216
26		*n* = 4	5246
27		*n* = 5	8319

[a] IC_{50}s are an average of at least two independent titrations.

core was prepared via a [3+2] cycloaddition between azides **10**[15] and 2-cyanoacetamide. Following removal of the NH_2 group with *tert*-butyl nitrite, the amide was dehydrated with TFAA to generate nitrile **17**. Next, the nitrile was reacted with sodium azide to afford the corresponding tetrazole, which after alkylation with ethyl bromoacetate, separation of the regioisomers[16] and hydrolysis of the ester led to desired compound **20**. Unfortunately, this modification resulted in a significant lost of SCD inhibitory activity (Table 1). Based on our previous inhibitors, which contain a piperazine or piperidine ring between the phenyl group and the heterocycle core (Fig. 1), we believed that **20** may be too short in length.

To this end, we decided to vary the number of carbons at the benzylic position. Syntheses of analogues **21** and **22**, using the appropriate benzyl bromide,[17] are show in Scheme 1. The rSCD data demonstrated that increasing the number of carbons at the benzylic position from 1 to 3 gave a modest improvement in the enzyme activity (Table 1).

Next, we explored different acetic acid chain lengths. To simplify the chemistry and avoid the difficult separation of the regioisomers generated in the alkylation step, we replaced the tetrazole heterocycle by an oxadiazole ring, which was previously found to be equipotent and a good replacement for the tetrazole moiety.[18] In addition, oxadiazole-acid inhibitors have demonstrated liver-

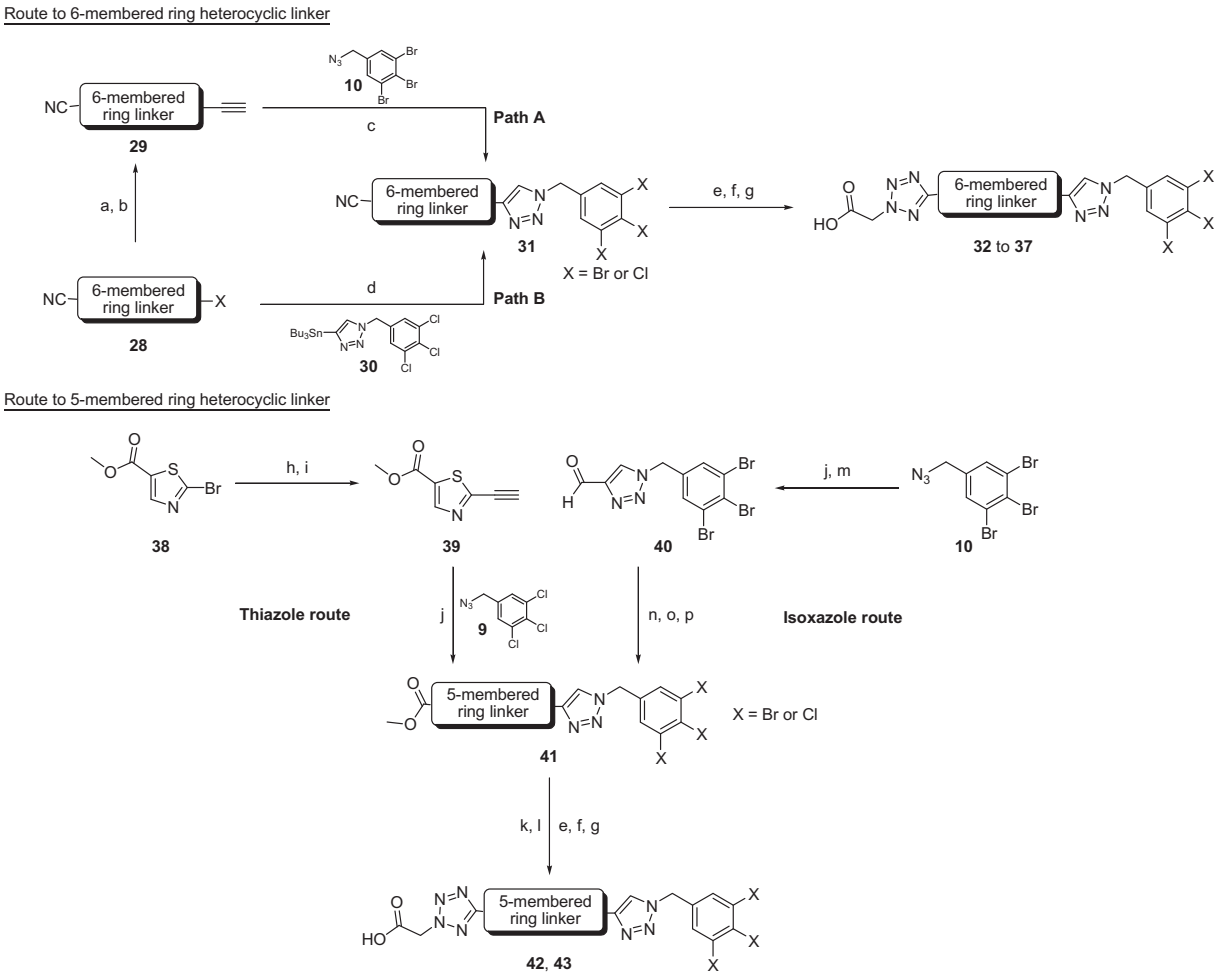

Scheme 2. Reagents and conditions: (a) ethynyl(trimethyl)silane, $Pd(PPh_3)_4$, CuI, DCM, TEA, 50 °C, 2 h; (b) TBAF, THF, rt, 30 min; (c) L-ascorbic acid sodium salt, copper(II) sulfate·$5H_2O$, THF, water, 60 °C, 16 h; (d) **30**, $Pd(PPh_3)_2Cl_2$, dioxane, reflux, 2.5 h; (e) NaN_3, NH_4Cl, DMF, 105 °C, 2 h; (f) ethyl 2-bromoacetate, TEA, THF, reflux, 2 h; (g) NaOH, THF, MeOH, rt, 3 h; (h) ethynyl(trimethyl)silane, $Pd(PPh_3)_4$, CuI, DCM, TEA, 50 °C, 2 h; (i) TBAF, THF, rt, 30 min; (j) L-ascorbic acid sodium salt, copper(II) sulfate·$5H_2O$, THF, water, 60 °C, 16 h; (k) NH_3, MeOH, 65 °C, 16 h; (l) TFAA, TEA, DCM, rt, 2 h; (m) DIBAL-H, DCM, −78 °C, 3 h; (n) NH_2OH·HCl, Na_2CO_3, THF, rt, 16 h; (o) NCS, DMF, rt, 20 h; (p) methyl propiolate, TEA, DMF, rt, 2.5 h.

Table 2
Effect of heterocyclic linkers

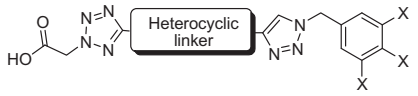

Compound	Heterocyclic linker	X	rSCD[a] (IC_{50}, nM)
32[c]	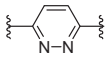	Cl	1814
33[b]	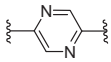	Br	1250
34[c]	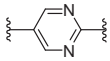	Cl	343
35[c]	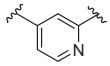	Cl	1314
36[c]	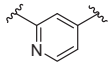	Cl	719
37[b]	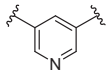	Br	56
42		Cl	49
43		Br	21

[a] IC_{50}s are an average of at least two independent titrations.
[b] Compounds were synthesis using path A in Scheme 2.
[c] Compounds were synthesis using path B in Scheme 2.

selective properties similar to tetrazole acetic acid inhibitors. Compounds **24**–**27** were synthesized from intermediate nitrile **17** in a three steps procedure using the appropriate acylchlorides[19] in the cycloaddition reaction (Scheme 1). As shown in Table 1, the optimum linker was obtained when a maximum of three carbons separate the acetic acid from the oxadiazole, but only with a modest improvement in potency.

Having observed that the length of the inhibitor has an effect on potency, we decided to explore more rigid heterocycles while keeping the tetrazole acetic acid and triazole moieties. We choose to begin our investigations by examining different six-membered ring linkers. As illustrated in Scheme 2, all the compounds from this series were accessed using path A or B.[14] In path A, the triazole core was generated via a Sharpless [3+2] cycloaddition[20] reaction between azide **10** and functionalized alkynes **29**. In path B, the preformed triazole core **30**[21] and the corresponding heterocyclic rings **28** were coupled under Stille reaction conditions. The few number of synthetic steps in this route allowed access to rapid analogue synthesis. Following standard procedures, the nitrile group was then converted into the tetrazole acetic acid to generate compounds **32**–**37**.

Initially, we decided to explore different substituted diazines (Table 2). However, modest activities were obtained, with IC_{50}s ranging from 1814 nM to 343 nM in the rSCD enzyme assay (**32**–**36**). Interestingly, we were pleased to observe an improvement in potency by changing the substitution angle pattern and the nature of the linker to pyridine (**37**). With regards to six-membered ring linkers, compound **37** showed the best result in the rat microsomal assay with an IC_{50} of 56 nM. This promising inhibitor was further tested in the rat hepatocyte assay[12] and in the HepG2 whole cell assay.[22] The more potent rat hepatocyte result over HepG2 data obtained with **37** suggest an active role of the OATPs and potentially a liver-targeted compound (Table 3).[23]

Indeed, mouse tissue distribution studies demonstrated good liver/tissue selectivity for **37**, in particular the liver-to-Harderian gland ratio (>94-fold, Table 3). Unfortunately, the mouse liver pharmacodynamic assay (mLPD)[24] showed no significant inhibition of SCD at a 30 mg/kg dose. We hypothesize that the low exposure observed in the liver (0.9 μM) is responsible for this lack of activity.

To address this issue, we decided to explore five-membered ring heterocyclic linkers. Given the success obtained with a thiazole and an isoxazole ring in our previous studies,[6,12] compounds **42** and **43** were synthesized (Scheme 2).[14] The thiazole analogue was accessed by building the triazole moiety on the alkyne **39** using a [3+2] cycloaddition with intermediate **9**. On the other hand, analogue **43** was accessed by building the isoxazole core on triazole intermediate **40** via a three steps synthesis using NH_4OH, NCS and methyl propiolate. Ester **41** was further converted to the desired final products using similar procedures as described previously.

The five-membered ring linker replacement maintained potency in the rat microsomal compared to the six-membered ring linker **37** (Table 3). Delightfully, **42** and **43** are liver-targeted with excellent liver-to-Harderian glands ratios of 66- and 100-fold, respectively, with compound **43** having the highest exposure in the liver in the mLPD. Unfortunately, even with a drug exposure of 8.4 μM, which is 40-fold above its rat hepatocyte potency, compound **43** did not afford any significant inhibition in the mLPD at a 30 mg/kg dose. We have examined activity across species (mouse, rat and human) for many SCD inhibitors and have found similar potencies.[12] Since IC_{50}s for **43** are similar in mouse (10 nM) and rat (21 nM), the lack of mLPD efficacy is not likely due to species differences. Although we do not completely understand this lack of efficacy, based on our experience with other liver-selective compounds, we observed that compounds with rat hepatocyte IC_{50}'s <200 nM and HepG2 IC_{50}'s <1000 nM are generally active in the

Table 3
Potency and efficacy of liver-targeted SCD inhibitors

Compound	In vitro[a]			In vivo		
	Rat microsomal	Rat hepatocyte	HepG2	Tissue distribution (10 mg/kg, 6 h po)		Mouse liver pharmacodynamic
	nM	nM	nM	[Liver] (μM)	Liver/Harderian glands ratio	[Liver] % inhibition at 30 mg/kg
5	19	10,106	760	2.7	0.4×	14 μM 46%[b]
37	56	694	6308	0.47	>94×	0.9 μM Not significant
42	49	975	>100,000	0.33	>66×	4.1 μM Not significant
43	21	212	37749	1.66	100x	8.4 μM 30%, Not significant

[a] IC_{50}s are an average of at least two independent titrations.
[b] Dose at 10 mg/kg.

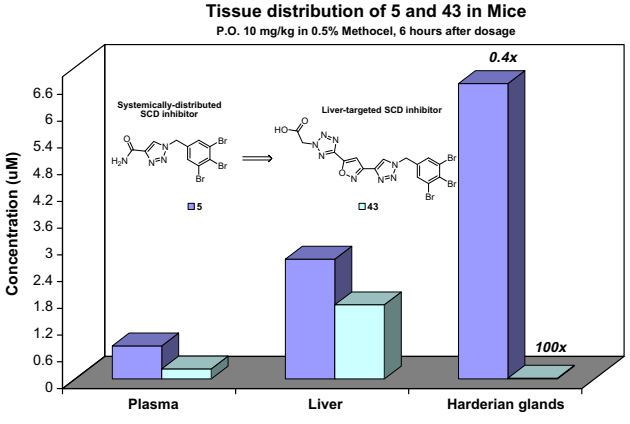

Figure 3. From systemic lead to liver-targeted inhibitor.

mLPD. It is likely that compounds **42** and **43** are too shifted in the HepG2 assay (IC_{50}'s >100,000 nM and 37,749 nM, respectively).

In summary, during an uHTS campaign we identified a structurally distinct class of potent SCD inhibitors. To avoid potential eye and skin adverse events, we converted the systemically distributed triazole-based compound **5** into liver-targeting inhibitors by the incorporation of a tetrazole acetic acid moiety and a pyridine linker (**37**). Further modifications of the middle ring linker allowed us to modulate in vitro (increased potency) and in vivo (increased liver exposure) properties and generated isoxazole **43**, a potent liver-selective SCD inhibitor (Fig. 3). Unfortunately, despite the good liver-selectivity and drug exposure, no significant in vivo inhibition was observed. Further studies are underway to identify more efficient and potent liver-targeting inhibitors of SCD in the mLPD.

Acknowledgments

The authors thank Dan Sørensen for NMR spectroscopic assistance on gHMBC, ^{15}N gHMBC and 1D NOESY experiments and Nicolas Lachance for his advice and suggestions.

References and notes

1. (a) Dobrzyn, P.; Dobrzyn, A. *Expert Opin. Ther. Patents* **2010**, *20*, 849; (b) Liu, G. *Expert Opin. Ther. Patents* **2009**, *19*, 1169; (c) Kopelman, P. G. *Nature* **2000**, *404*, 635.
2. Enoch, H. G.; Catala, A.; Strittmatter, P. J. *Biol. Chem.* **1976**, *251*, 5095.
3. Ntambi, J. M. *Prog. Lipid Res.* **1995**, *34*, 139.
4. (a) Jiang, G.; Li, Z.; Liu, F.; Ellsworth, K.; Dallas-Yang, Q.; Wu, M.; Ronan, J.; Esau, C.; Murphy, C.; Szalkowski, D.; Bergeron, R.; Doebber, T.; Zhang, B. B. J. *Clin. Invest.* **2005**, *115*, 1030; (b) Miyazaki, M.; Flowers, M. T.; Sampath, H.; Chu, K.; Otzelberger, C.; Liu, X.; Ntambi, J. M. *Cell Metab.* **2007**, *6*, 484; (c) Savransky, V.; Jun, J.; Li, J.; Nanayakkara, A.; Fonti, S.; Moser, A. B.; Steele, K. E.; Schweitzer, M. A.; Patil, S. P.; Bhanot, S.; Schwartz, A. R.; Polotsky, V. Y. *Circ. Res.* **2008**, *103*, 1173.
5. (a) Dobrzyn, A.; Ntambi, J. M. *Prostaglandins Leukot. Essent. Fatty Acids* **2005**, *73*, 35; (b) Dobrzyn, A.; Ntambi, J. M. *Obes. Rev.* **2005**, *6*, 169.
6. Li, C. S.; Belair, L.; Guay, J.; Murgasva, R.; Sturkenboom, W.; Ramtohul, Y. K.; Zhang, L.; Huang, Z. *Bioorg. Med. Chem. Lett.* **2009**, *19*, 5214.
7. Leger, S.; Black, C.; Deschenes, D.; Dolman, S.; Falgueyret, J.-P.; Gagnon, M.; Guiral, S.; Huang, Z.; Guay, J.; Leblanc, Y.; Li, C.-S.; Masse, F.; Oballa, R.; Zhang, L. *Bioorg. Med. Chem. Lett.* **2010**, *20*, 499.
8. (a) Xin, Z.; Zhao, H.; Serby, M. D.; Liu, B.; Liu, M.; Szczepankiewicz, B. G.; Nelson, L. T.; Smith, H. T.; Suhar, T. S.; Janis, R. S.; Cao, N.; Camp, H. S.; Collins, C. A.; Sham, H. L.; Surowy, T. K.; Liu, G. *Bioorg. Med. Chem. Lett.* **2008**, *18*, 4298; (b) Winther, M. D. 2nd Annual Drug Development for Diabetes and Obesity, London, UK, Jan 17–18, 2008.; (c) Koltun, D. O.; Vasilevich, N. I.; Parkhill, E. Q.; Glushkov, A. I.; Zilbershtein, T. M.; Mayboroda, E. I.; Boze, M. A.; Cole, A. G.; Henderson, I.; Zautke, N. A.; Brunn, S. A.; Chu, N.; Hao, J.; Mollova, N.; Leung, K.; Chisholm, J. W.; Zablocki, J. *Bioorg. Med. Chem. Lett.* **2009**, *19*, 3050; (d) Uto, Y.; Ogata, T.; Kiyotsuka, Y.; Miyazawa, Y.; Ueno, Y.; Kurata, H.; Deguchi, T.; Yamada, M.; Watanabe, N.; Takagi, T.; Wakimoto, S.; Okuyama, R.; Konishi, M.; Kurikawa, N.; Kono, K.; Osumi, J. *Bioorg. Med. Chem. Lett.* **2009**, *19*, 4159; (e) Ramtohul, Y. K.; Black, C.; Chan, C.-C.; Crane, S.; Guay, J.; Guiral, S.; Huang, Z.; Oballa, R.; Xu, L.-J.; Zhang, L.; Li, C. S. *Bioorg. Med. Chem. Lett.* **2010**, *12*, 23; (f) Powell, D. A.; Ramtohul, Y. K.; Lebrun, M.-E.; Oballa, R.; Falgueyret, J.-P.; Guiral, S.; Huang, Z.; Skorey, K.; Tawa, P.; Zhang, L. *Bioorg. Med. Chem. Lett.* **2010**, *20*, 6366; (g) ACS 240th, Boston, 2010.; (h) Isabel, E.; Powell, D. A.; Black, C.; Chan, C.-C.; Crane, S.; Gordon, R.; Guay, J.; Guiral, S.; Huang, Z.; Robichaud, J.; Skorey, K.; Tawa, P.; Xu, L.; Zhang, L.; Oballa, R. *Bioorg. Med. Chem. Lett.* **2011**, *21*, 479; (i) Atkinson, K. A.; Beretta, E. E.; Brown, J. A.; Castrodad, M.; Chen, Y.; Cosgrove, J. M.; Du, P.; Litchfield, J.; Makowski, M.; Martin, K.; McLellan, T. J.; Neagu, C.; Perry, D. A.; Piotrowski, D. W.; Steppan, C. M.; Trilles, R. *Bioorg. Med. Chem. Lett.* **2011**, *21*, 1621.
9. (a) Five initial applications from Xenon (WO2005/011653 to WO 2005/011657) were published on February 10, 2005. WO2008/074835 and WO2009/106991 were also published in 2008 and 2009 respectively. Representative one: Abreo, M.; Chafeev, M.; Chakka, N.; Chowdhury, S.; Fu, J.-M.; Gschwend, H. W.; Holladay, M. W.; Hou, D.; Kamboj, R.; Kodumuru, V.; Li, W.; Liu, S.; Raina, V.; Sun, S.; Sun, S.; Sviridov, S.; Winther, M. D.; Zhang, Z. WO2005/011655.; (b) Xenon/Novartis patent: Dales, N.; Zhang, Z. WO2008/024390.; (c) Three patents from GSK in 2009: WO2009/016216, WO2009/060053 and WO2009/060054. Representative one: Bouillot, A. M. J.; Laroze, A.; Trottet, L. WO2009/060053.
10. Our approach was based on a SPA technology and recombinant FLAG tag human SCD-1. In the first screen of the sample collection, a binding assay was used to identify novel chemical structures, as well as the design of selective and potent human SCD-1 inhibitors. Over 1.6×10^6 compounds were tested and 12109 were found to give >35% inhibition at 9 μM. After confirmation of the potency (triplicate of the binding assay), compounds were filtered, clustered and then tested in a rat microsomal assay using a 3 point titration. Finally, the best compounds were retested in the same rat assay using a 10 point titration curve. For more details see Skorey, K. and co-worker, *J. Biomol. Screen.* **2011**, *16*, 506.
11. For rat microsomal assay conditions, see: Li, C. S.; Ramtohul, Y.; Huang, Z.; Lachance, N. WO2006/130986.
12. Oballa, R. M.; Belair, L.; Black, C.; Bleasby, K.; Chan, C. C.; Desroches, C.; Du, X.; Gordon, R.; Guay, J.; Guiral, S.; Hafey, M. J.; Hamelin, E.; Huang, Z.; Kennedy, B.; Lachance, N.; Landry, F.; Li, C. S.; Mancini, J.; Normandin, D.; Pocai, A.; Powell, D.; Ramtohul, Y.; Skorey, K.; Sturkenboom, W.; Styhler, A.; Waddleton, D.; Wang, H.; Wong, S.; Xu, L.; Zhang, L. *J. Med. Chem.* **2011**, *54*, 5082.
13. For a review on OATP transporters, see: Niemi, M. *Pharmacogenomics* **2007**, *8*, 787.
14. For detailed experimental procedures, see: Leclerc, J.-P.; Li, C. S.; Ramtohul, Y. K. WO 2010/025553.
15. For detailed experimental procedures on the synthesis of azide **10**, see: Strassburg, R. W.; Gregg, R. A.; Walling, C. *J. Am. Chem. Soc.* **1947**, *69*, 2141.
16. *N*2-Tetrazole acetic acid substitution showed reduced activity over the *N*3-tetrazole acetic acid regioisomer. The proper regiochemistry was confirmed by evaluation of the structures through NMR experiments: gHMBC, ^{15}N gHMBC and 1D NOESY.
17. For detailed experimental procedures on the synthesis of azides **11** and **12**, see: (a) Blankespoor, L. R.; DeVries, T.; Hansen, E.; Kallemeyn, M. J.; Klooster, M. A.; Mulder, A. J.; Smart, P. R.; Vander Griend, A. D. *J. Org. Chem.* **2002**, *67*, 2677; (b) Katzenellenbogen, A. J.; Robertson, D. W. *J. Org. Chem.* **1982**, *47*, 2387.
18. Unpublished results.
19. For detailed experimental procedures on acylchloride syntheses, see: (a) Thompson, A.; Regourd, J.; Al-Sheikh Ali, A. *J. Med. Chem.* **2007**, *50*, 1528; (b) Shiraishi, M.; Kato, K.; Terao, S.; Ashida, Y.; Terashita, Z.-I.; Kito, G. *J. Med. Chem.* **1989**, *32*, 2214.
20. Rostovtsev, V. V.; Green, L. G.; Fokin, V. V.; Sharpless, K. B. *Angew. Chem., Int. Ed.* **2002**, *41*, 2596.
21. Intermediate **30** was obtained from the reaction of azide **9** with ethynyltri-*N*-butyltin in benzene at 80 °C for 5 h.
22. Zhang, L.; Ramtohul, Y.; Gagné, S.; Styhler, A.; Guay, J.; Huang, Z. *J. Biomol. Screen.* **2010**, *15*, 169.
23. Active OATPs are present in the cells of the rat hepatocyte assay, as opposed to the HepG2 whole cells which lack these active transporters. When compared side by side, those two assays give a good indication of potential active drug transport in the liver as compared to passive cell diffusion. As such, a liver-targeted SCD inhibitor transported by the OATPs will have a more potent hepatocyte IC_{50} values over HepG2 inhibition. Therefore, this can be use to evaluate the potential liver-targeted nature of a compound before performing pharmacokinetic studies.
24. Mouse liver pharmacodynamic model (mLPD) is expressed in percentage (%) inhibition and is used to assess the in vivo potency. In the mLPD experiment, mice (male C57BL6) were fed on a high carbohydrate diet and the SCD activity was indexed 3 h post oral dose of SCD inhibitors by following the conversion of intravenously administered [1-^{14}C]-stearic acid tracer to the SCD-derived [1-^{14}C]-oleic acid in liver lipids. The percentage (%) of inhibition of an SCD inhibitor is calculated from the liver SCD activity index (ratio of ^{14}C-oleic acid/^{14}C-stearic acid) from drug treated animals compared to a vehicle group.